Adsorption of dark compounds with bentonites in apple juice

Hülya Koyuncu[a,*], Ali Rıza Kul[b], Ayla Çalımlı[c], Nuray Yıldız[c], Hasan Ceylan[b]

[a]*Department of Food Engineering, Faculty of Agriculture, Yuzuncu Yil University, 65080 Van, Turkey*
[b]*Department of Chemistry, Faculty of Art and Science, Yuzuncu Yil University, 65080 Van, Turkey*
[c]*Department of Chemical Engineering, Faculty of Engineering, Ankara University, 06100 Tandoğan, Ankara, Turkey*

Abstract

The adsorption equilibrium of dark-coloured compounds from apple juice has been investigated as a function of several variables including activation conditions of bentonite (heat and acid treatments), clay concentrations (2×10^{-3}–8×10^{-3} kg clay/dm^3 apple juice) and temperature (range of 296–336 K). The adsorption efficiency with acid-activated bentonite was greater than that with heat-activated and native bentonite, depending on surface properties; specific surface areas were 95.31, 71.95 and 71.76 m^2/g, respectively.

Absorbance data at 420 nm were fitted reasonably well with the Langmuir and Freundlich isotherms. The parameters K, Q_0, K_{fr} and n were determined for different temperatures. Thermodynamic parameters such as Gibbs free energy (ΔG), enthalpy (ΔH) and entropy (ΔS) change of adsorption were determined as about -3.125, 9.43 and 0.039 kJ mol^{-1} K^{-1}, respectively, for acid-activated bentonite. These parameters were also determined for native and heat-activated bentonites. It was shown that the adsorption process was endothermic, spontaneous and controlled by physical mechanism. The adsorption and desorption rate constants (k_a and k_d) were obtained separately by applying a geometric approach to the first-order Langmuir model. k_a varied from 5.717×10^{-4} to 20.667×10^{-3} s^{-1} and k_d from 1.425×10^{-4} to 7.473×10^{-3} s^{-1}. The results showed that acid-activated bentonite is more suitable for the adsorption of dark compounds from apple juice.

1. Introduction

Apples are the most widely grown and consumed of fruit in the world (Lea, 1990; Root, 1996). During processing of apple juice and also during storage, some alterations in apple juice composition can occur. One of the most important change is enzymatic and not enzymatic browning (González, Ibarz, Esplugas, & Vincente, 1998; Ibarz, Casero, Miguelsanz, & Pagán, 1989; Toribio & Lozano, 1984). In order to prevent apple juice from browning and haze formation, and in many cases to optimize taste characteristics, a deliberate reduction of phenolics is necessary (Constenla & Lozano, 1995; Giovanelli & Ravasini, 1993). Various pre- and post-treatments are now available to avoid the risk of post-turbidity and

colouration of apple juices. Stabilization of beverages by means of gelatine, bentonite, activated carbon and silica gel is a widespread, conventional treatment in the juice industry (Artık, Cemeroğlu, & Aydar, 1994; Babsky, Toribio, & Lozano, 1986; Beveridge, Franz, & Harrison, 1986; Dik & Özilgen, 1994). Polyvinylpolypyrrolidone (PVPP) has also been established in recent years as a final stabilization treatment (Günter & Stocké, 1995; Hums, Krug, Heess, & Storz, 1980; Vogt, 1987). Similarly, the use of adsorbent resins for the stabilization of clear apple juice has gained an increasing importance as a final treatment after clarification (Gökmen & Serpen, 2002; Schobinger, Barbic, Dürr, & Waldvogel, 1995; Weinand, 1995). Bentonites are used to clarify apple juice. The major clarification mechanism is adsorption on the surface, which removes proteins, heavy metal ions, pesticides and dark compounds (Blade & Boulton, 1988; Carabasa, Ibarz, Garza, & Barbosa-Cánovas, 1998; Dik, Katnaş & Özilgen, 1996; Ekşi, 1988). Bentonites have a layered crystalline

*Corresponding author. Tel.: +90 432 2251002/1669; fax: +90 432 2251104.

E-mail address: hkoyuncu@yyu.edu.tr (H. Koyuncu).

Nomenclature

A_0, A initial absorbance, final absorbance
$A_{a,d}$ frequency factor of adsorption and desorption
C (dimensionless) equilibrium concentration of the fluid phase
E_a (kJ mol^{-1}) activation energy of adsorption
E_d (kJ mol^{-1}) activation energy of desorption
k_0 (s^{-1}) initial adsorption rate
k_a (s^{-1}) adsorption rate constant
K adsorption equilibrium constant
k_d (s^{-1}) desorption rate constant
K_{fr} (kg^{-1}) Freundlich constant
m (kg) amount of bentonite

n Freundlich constant
Q (kg^{-1}) equilibrium concentration of the adsorbate in the adsorbing phase
Q_0 (kg^{-1}) maximum concentration retained by the adsorbent
R (J mol^{-1} K^{-1}) universal gas constant
t (s)   time
t_{ie} (s) initial equilibrium time
T (K)   absolute temperature
θ coverage fraction
θ_e equilibrium coverage fraction
ΔG (kJ mol^{-1}) Gibbs free energy
ΔH (kJ mol^{-1}) enthalpy change
ΔS (kJ mol^{-1} K^{-1}) entropy change

---

structure made up of two outer silica sheets and a central sheet of aluminium ions. Water and the exchangeable calcium and sodium cations are located within the sheets. Adsorption capability of bentonites increases with their swelling capability in water. The acid and heat treatments for activation of bentonites change structural/textural properties of bentonites (Venaruzzo, Volzone, Rueda, & Ortiga, 2002).

The aim of the present investigation is to study the adsorption mechanism of dark-coloured compounds from apple juice onto native, heat-activated and acid-activated bentonite, and determination of the equilibrium and kinetic parameters. Towards this aim, the adsorption isotherms at different temperatures, Langmuir and Freundlich adsorption model parameters and thermodynamic parameters of these adsorption processes were determined. The adsorption and desorption rate constants and the other kinetic constants such as the activation energies of adsorption and desorption and frequency factors were determined separately by geometric approach.

1.1. Equilibrium and kinetic models

The adsorption isotherms express the relationships between equilibrium concentrations of the adsorbate in the adsorbing phase (Q) and fluid phase (C) at a fixed temperature. The linear form of Langmuir (1918) model can be expressed as

$$1/Q = 1/Q_0 + 1/(Q_0 K C), \tag{1}$$

where Q_0 is the maximum concentration retained by the adsorbent surface and K is the adsorption equilibrium constant.

The linear form of Freundlich adsorption model can be expressed as

$$\ln Q = ln\,K_{fr} + n\,\ln C, \tag{2}$$

where K_{fr} and n are Freundlich constants.

In this study, a geometric approach described by Kuan, Lo, Chang, and Wang (2000) was applied to separately

determine adsorption and desorption constants. A typical plot of θ (Q/Q_0) versus time (t) relationship can be obtained, resulting from a conventional kinetic experiment. The curve can be divided into an initial fast reaction interval and a later slow reaction interval. A linear regression analysis of data collected from the early stage will yield a slope k_0, namely the initial adsorption rate, and the intercept of linearization of data in the later stage gives the equilibrium coverage fraction (θ_e). Initial equilibrium time t_{ie}, k_a and k_d can be expressed as (Kuan et al., 2000)

$$t_{ie} = \theta_e/k_0, \tag{3}$$

$$k_a = 2k_0/C, \tag{4}$$

$$k_d = 2(1 - k_0 t_{ie})/t_{ie}. \tag{5}$$

The adsorption and desorption activation energies can be calculated according to the linear form of Arrhenius equation:

$$\ln k_a = \ln A_a - E_a/RT, \tag{6}$$

$$\ln k_d = \ln A_d - E_d/RT, \tag{7}$$

where E_a and E_d represent the activation energy of adsorption and desorption, respectively. A_a and A_d are the adsorption and desorption frequency factors, respectively; R is the universal gas constant and T is the absolute temperature.

2. Materials and methods

2.1. Activation treatments of bentonite

The bentonite samples used in this study were obtained from Kütahya region in Turkey (chemical analysis in Table 1). In order to increase the surface area and provide physico-chemical changes in the structure of bentonite, heat and acid activation tests were performed.

In the heat activation, 0.050 kg of native bentonite was placed in a furnace (SFL, Seven Furnaces Limited) at 773 K for a period of 72×10^3 s. Then the sample was

Table 1
Chemical analysis of Kütahya bentonite

	SiO_2	Al_2O_3	Fe_2O_3	TiO_2	CaO	MgO	Na_2O	K_2O	KK[a]	Others
g/100 g	71.600	13.150	0.660	0.070	2.230	2.790	0.260	0.360	8.450	0.430

[a]Weight loss at 1000 °C.

sieved by 235-mesh sieve (61.75 μm) and then put into a desiccator.

The acid treatment was carried out using a pyrex glass reactor with reflux condenser. The reactor was placed onto Chiltern Hotplate Magnetic Stirrer HS 31. Native bentonite (0.050 kg) was slowly added to 0.25 dm³ of 5 mol/dm³ HCl solution, stirred and maintained at boiling temperature (approximately 378 K) during 10.8×10^3 s. After treatment, the reaction products were filtered and 15 times washed with distilled water to remove traces of acid. After each washing, Cl^- ions were detected with silver acetate solution and then the sample was centrifuged with MSE MISTRAL 2000 at 4500 rpm for 300 s. The final sample was centrifuged and kept at 333 K in an oven (Philip Harris Ltd.) to remove some of the moisture, for 172.8×10^3 s for complete drying. The sample was milled by passing through 235-mesh sieve (61.75 μm) to eliminate the formation of lumps produced during drying, and saved in a desiccator.

Adsorption equilibrium and kinetic studies were performed with native, heat- and acid-activated bentonite.

2.2. BET analysis

Specific surface areas (BET) and pore-size distributions of the original and activated bentonite samples were determined using a Quantachrome NOVA 2200 series volumetric gas adsorption instrument. The determinations were based on measurements of the corresponding nitrogen adsorption isotherms at 77 K. Before measurements were started, moisture and gases such as nitrogen and oxygen that were adsorbed on the solid surface or held in the open pores were removed under reduced pressure at 423 K for 18×10^3 s.

2.3. Preparation of the apple juice

In this study, Golden delicious variety, which grows in Van cast region in Turkey like anywhere in the world, was used. A local variety of Golden delicious was purchased in the local market in Van. After washing, sorting and cutting into pieces, apple juice was prepared with a typical home juicer (Arcelik Robopress model ARK-71 RP, Turkey). The raw apple juice was treated with 0.1% pectinase (Pectinex 3XL, Novo, Denmark) (2.5×10^{-3} dm³ enzyme/ dm³ apple juice). The enzymatic treatment was performed for 10.8×10^3 s at 323 K. After this treatment, the alcohol test applied for depectinization was exactly completed. The enzyme-treated apple juice was filtered through a black

band filter paper by using suction flask. Total soluble solids content, which was measured by a hand-type refractometer, and pH of the depectinized juice were 13.1°Brix and 4.24, respectively. The apple juice was diluted to 11°Brix by bi-distilled water.

The bentonites were hydrated in bi-distilled water (10 dm³ water/kg clay) at room temperature for 61.2×10^3 s. Then the hydrated bentonites were filtered using gooch filter with vacuum, and net weights of the hydrated bentonites were calculated.

For the adsorption equilibrium studies, the bentonites (native, heat- and acid-activated) at amounts of 2×10^{-5}, 4×10^{-5} and 8×10^{-5} kg on dry basis were combined with 10×10^{-3} dm³ of 11°Brix apple juice in glass flasks to obtain bentonite concentrations of 2×10^{-3}, 4×10^{-3} and 8×10^{-3} kg clay/dm³ apple juice, respectively. All flasks were put in an incubator at fixed temperatures (296, 316 and 336 K), and shaken for up to 57.6×10^3 s to reach the equilibrium conditions. All absorbance measurements were performed using LKB Biochrom Ultrospec 4050 model spectrophotometer at 420 nm. A flask containing 10×10^{-3} dm³ of apple juice (no clay) was used as a control sample and the initial absorbance value (A_0) was determined with this sample at 420 nm. The measurement of absorbance at 420 nm gives an idea of melanoidin content (dark-coloured compounds). For the adsorption kinetic studies, changes of absorbance at 420 nm were determined at 300, 600, 900, 1200, 1500, 1800, 3600, 7200, 18×10^3, 14.4×10^3, 21.6×10^3 and 57.6×10^3 s during the adsorption process at three different temperatures (296, 316 and 336 K) with the bentonite concentrations indicated above. All absorbance measurements for adsorption process were corrected with the control sample for each corresponding time intervals in order to exclude thermal and storage effects on measured absorbance.

3. Results and discussion

In preliminary tests, it was found that 57.6×10^3 s is enough to reach the dynamic equilibrium between fluid phase (apple juice) and solid phase (bentonite).

3.1. Surface area and pore distribution of samples

Adsorption isotherms of N_2 at 77 K for the native and activated samples of bentonite are illustrated in Fig. 1. The general shape of the isotherm stayed at the same. The nitrogen volume adsorbed by heat-activated bentonite is higher at relative pressure of 0.9 (cm³/g), than that of
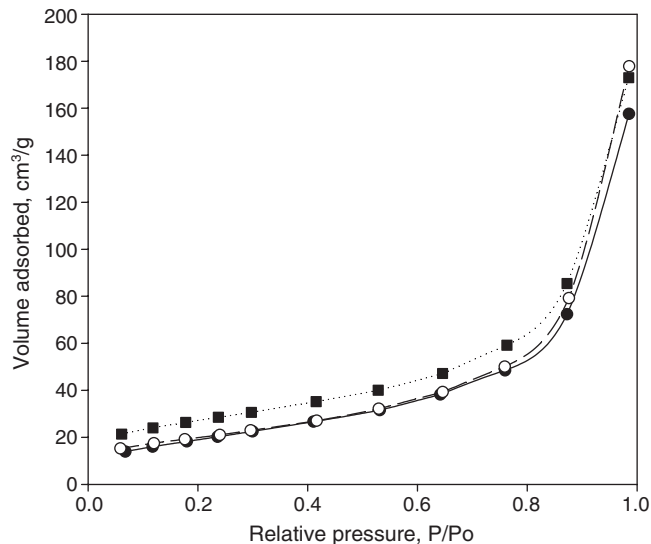
Fig. 1. Adsorption isotherms of nitrogen at 77 K of the native and activated bentonite samples: ♦ = native bentonite, ■ = heat-activated bentonite, ○ = acid-activated bentonite.

Fig. 2. Pore-size distributions for the native and activated bentonite samples: ♦ = native bentonite, ■ = heat-activated bentonite, ○ = acid-activated bentonite.

Fig. 3. The effect of acid-activated bentonite concentration and temperature on the adsorption (%) in apple juice at 420 nm: ♦ = 296 K, ■ = 316 K, ▲ 336 K.

native and acid-activated bentonite Fig. 1. The specific surface areas of the samples were calculated from nitrogen adsorption isotherms by the BET method, mainly for comparative purposes.

The acid activation causes formation of smaller pores in solid particles, resulting in higher surface area (95.31 m²/g) relative to original and thermal-activated bentonite (71.95 and 71.76 m²/g, respectively). Similar results were also obtained by Jovanovic and Janackovie (1991) and Yıldız, Aktaş, and Çalımlı (2004).

For a textural characterization of any porous solid, the concept of surface area does not give a visual picture of it. Pore size and pore-size distributions are necessary if the material has to be fully characterized. The pore-size distribution in the mesopore region was obtained by applying the method of BJH (Barrett, Joyner, & Halenda, 1951) to the desorption brunch of the isotherms of nitrogen at 77 K, assuming the pores to be cylindrical in shape.

Fig. 2 compares the change of pore-size distribution for native and activated samples. As seen from the figure, the samples have mesopores of which diameters are between 20 and 500 Å. While the original and heat-activated samples exhibited maximum differential pore volumes at about 39 Å in pore diameter, for acid-activated bentonite it was 35 Å. When the pore diameter decreases below 35 or 39 Å, the differential pore volumes for these samples tend to decrease.

3.2. Adsorption efficiencies

The adsorption efficiencies of dark-coloured compounds contained in apple juice on native and activated bentonite samples were evaluated by determining the percentage decrease of the absorbance at 420 nm of the juice by using the following equation as previously expressed
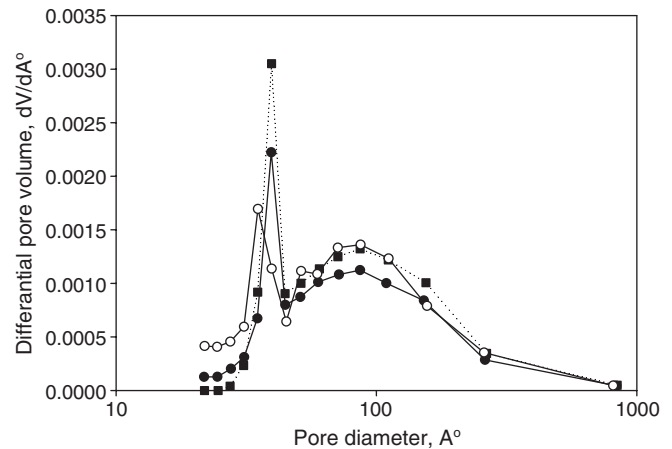
by Carabasa et al. (1998):

$$Adsorption\ (\%) = [(A_0 - A)/A_0] \times 100, \qquad (8)$$

where A_0 is the initial absorbance at 420 nm and A is the final absorbance at 420 nm. The variation of adsorption (%) with the concentration of the acid-activated bentonite in the apple juice (m, kg clay/dm³ apple juice) at various treatment temperatures is shown in Fig. 3. It can be seen that the adsorption efficiency increases with increasing temperature. Similar results have been reported by Gökmen and Serpen (2002) for the adsorption of dark-coloured compounds from apple juice, using adsorbent resin. On the other hand, an increase of adsorption efficiency with increasing concentration of bentonite in the apple juice was observed for native and activated bentonite because the available adsorption surface was increased. As seen from Figs. 3–5, the adsorption efficiency with acid-activated bentonite was greater than that with heat-activated and
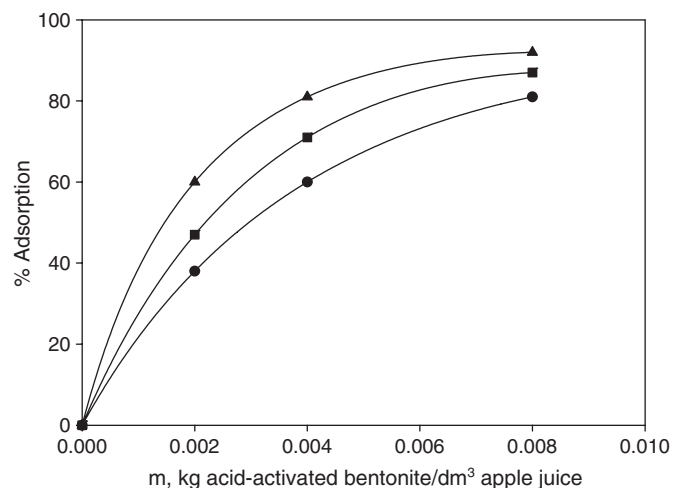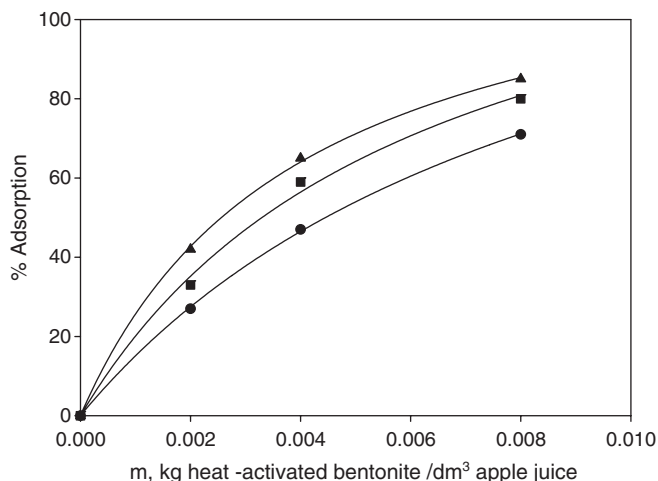
Fig. 4. The effect of heat-activated bentonite concentration and temperature on the adsorption (%) in apple juice at 420 nm: ♦ = 296 K, ■ = 316 K, ▲ 336 K.

Fig. 6. The adsorption isotherms of dark-coloured compounds on the acid-activated bentonite at different temperatures: ♦ = Experimental (296 K), − = Langmuir (296 K), ■ = Experimental (316 K), − = Langmuir (316 K), ▲ = Experimental (336 K), − = Langmuir (336 K).

Table 2
Langmuir parameters at different temperatures for native, heat-activated and acid-activated bentonite

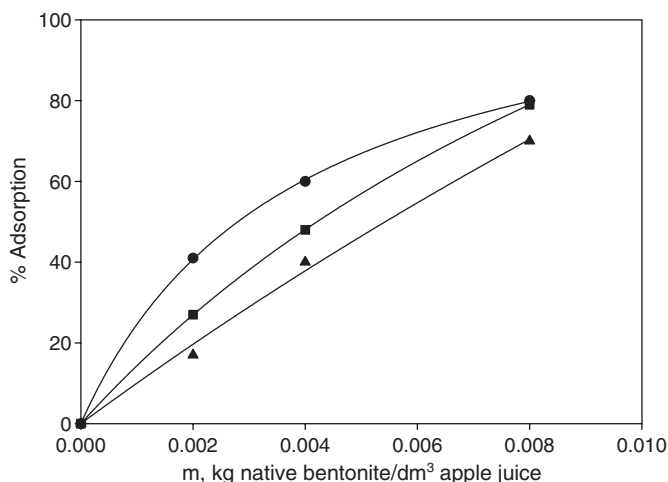| Bentonite	T (K)	Q_0 (1/kg clay)	K	r^2
Native	296	187	1.874 ± 0.373	0.998
	316	223	2.158 ± 0.202	0.998
	336	298	2.357 ± 0.084	0.992
Heat-activated	296	202	2.693 ± 0.132	0.998
	316	243	3.526 ± 0.107	0.994
	336	300	3.630 ± 0.041	0.994
Acid-activated	296	294	2.744 ± 0.023	0.995
	316	374	3.152 ± 0.071	0.999
	336	487	3.852 ± 1.728	0.999

Fig. 5. The effect of native bentonite concentration and temperature on the adsorption (%) in apple juice at 420 nm: ♦ = 296 K, ■ = 316 K, ▲ = 336 K.

native bentonite. The maximum values of the adsorption efficiency for native, heat-activated and acid-activated bentonite were found as 80%, 85% and 92%, respectively, for 8×10^{-3} kg clay/dm³ apple juice at 336 K.

3.3. Adsorption isotherms

The analysis of the isotherm data by fitting them into different isotherm models is an important step to find the suitable model that can be used for design process. In this study, the dimensionless forms of isotherms are studied (Carabasa et al., 1998; Gökmen & Serpen, 2002). Fig. 6 shows a plot of Q versus C for acid-activated bentonite, where C (A/A_0) represents the liquid phase absorbance at 420 nm and Q ($[(A_0-A)/A_0]/m$) represents the solid phase absorbance at 420 nm, where m is the amount of bentonite.
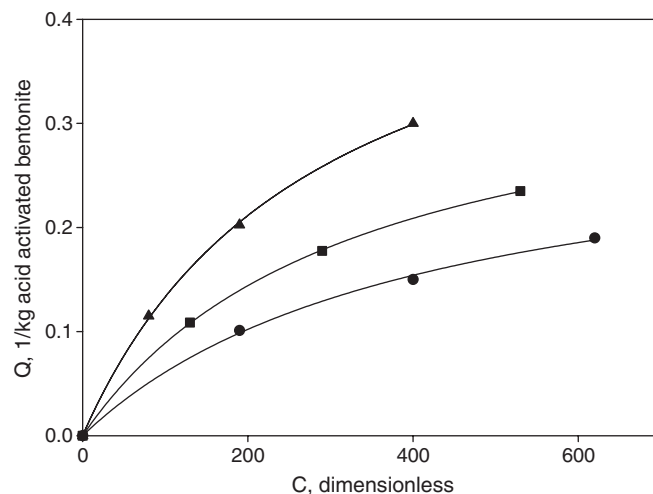
The curves of native and heat-activated bentonite were similar to the curve of acid-activated bentonite showed in Fig. 6. These types of isotherms (convex upward) are designated as favourable type (McCabe, Smith, & Harriott, 1993).

3.4. Adsorption models

The adsorption data for the natural, heat- and acid-activated bentonites were fitted to linear form of the Langmuir model Eq. (1). The intercept of lines at $1/Q$ axis gives $1/Q_0$ and the slope of lines gives $1/KQ_0$. The maximum adsorption capacity (Q_0), the adsorption equilibrium constant (K) and correlation coefficient (r^2) for the three kinds of bentonites are given in Table 2. The adsorption capacities (Q_0) and the adsorption equilibrium constants (K) were observed to increase with increasing temperature, showing the adsorption process to be endothermic.

The fitting of the experimental data to the linear form of the Freundlich model Eq. (2) were also performed. K_{fr} and n are determined from the intercept and the slope of the plot $\ln Q$ versus $\ln C$, respectively. As shown in Table 3, in all the assays, the Freundlich parameters K_{fr} and n were increased with increasing temperature (Carabasa et al., 1998; Gökmen & Serpen, 2002).

3.5. Thermodynamic evaluation of the adsorption process

Thermodynamic parameters such as Gibbs free energy (ΔG), enthalpy change (ΔH) and entropy change (ΔS) for the adsorption of dark-coloured compounds onto native, heat- and acid-activated bentonite are given in Table 4. ΔG is calculated using the following equation:

$$\Delta G = -RT \ln K, \qquad (9)$$

where K is the adsorption equilibrium constant (from Langmuir model), T is the absolute temperature and R is the universal gas constant. The relation between K and the thermodynamic parameters of ΔH and ΔS can be described by Van't Hoff correlation in the following equation:

$$\ln K = (\Delta S/R) - (\Delta H/RT). \qquad (10)$$

ΔH and ΔS were calculated from the slope and intercept of Van't Hoff plots, respectively. As evident from Table 4, the positive values of ΔH indicated the endothermic nature of adsorption of dark-coloured compounds onto native, heat- and acid-activated bentonite. In addition, the enthalpy of adsorption for each bentonite sample is lower than $40\,kJ\,mol^{-1}$, indicating that the adsorption processes were controlled by physical mechanism rather than chemical mechanism (Ajmal, Rao, Ahmad, & Ahmad, 2000; Kara, Yuzer, Sabah, & Celik, 2003; Özcan, Erdem, & Özcan, 2004; Tahir & Rauf, 2003). The negative values of Gibbs free energy of adsorption (ΔG) indicated that the adsorption of dark-coloured compounds onto the clay surfaces was spontaneous. The decrease in ΔG with rise in temperature shows that the reaction is more favourable at higher temperatures (Tahir & Rauf, 2003; Yıldız, Gönülşen, Koyuncu, & Çalımlı, 2005). Since the adsorption is endothermic, the adsorption process is therefore made spontaneous because of positive entropy-change. The positive values of ΔS indicated the increased randomness at the solid/solution interface during the adsorption of dark-coloured compounds onto the bentonites. Similar results have been reported by Gökmen and Serpen (2002). The adsorption process is composed of enthalpic and entropic contributions (Kara et al., 2003). Examination of Table 4 reveals that ΔH is rather larger compared to the total adsorption energy. However, the entropic contributions are even smaller than the Gibbs free energy of adsorption. Therefore, it is to say that the adsorption of dark-coloured compounds onto the clays is enthalpic governed.

3.6. Adsorption kinetics

Fig. 7 shows a typical example of the plot of coverage fraction (θ) versus time (t), using the data from batch kinetic experiments. The data (θ vs t) were fitted to a growth model [$\theta = a(b - e^{-ct})$], where a, b and c are constants which were calculated by using the software package programme of Curve Expert version 1.3. The derivative of the growth model function at $t = 0$ ($d\theta/dt = ac$) yielded the initial adsorption rate (k_0). The

Table 3
Freundlich parameters at different temperatures for native, heat-activated and acid-activated bentonite

Bentonite	T (K)	K_{fr} (1/kg clay)	n	r^2
Native	296	126	0.495 ± 0.068	0.989
	316	161	0.496 ± 0.035	0.985
	336	225	0.512 ± 0.014	0.969
Heat-activated	296	157	0.468 ± 0.012	0.999
	316	206	0.437 ± 0.005	0.969
	336	276	0.504 ± 0.001	0.999
Acid-activated	296	245	0.533 ± 0.007	0.999
	316	340	0.551 ± 0.001	0.994
	336	528	0.597 ± 0.042	0.996

Table 4
Thermodynamic parameters for the adsorption process of dark coloured compounds onto native, heat-activated and acid-activated bentonite

Bentonite	T (K)	K	ΔG (kJ mol^{-1})	ΔH (kJ mol^{-1})	ΔS (kJ mol^{-1}K^{-1})	r^2
Native	296	1.874	−1.476			
	316	2.158	−2.022	8.277	0.032	0.987
	336	2.357	−2.514			
Heat-activated	296	2.693	−2.436			
	316	3.526	−3.152	8.511	0.036	0.943
	336	3.630	−3.632			
Acid-activated	296	2.744	−2.484			
	316	3.152	−3.016	9.435	0.039	0.995
	336	3.852	−3.768			

initial equilibrium time (t_{ie}) was then calculated using Eq. (3). The equilibrium coverage fraction (θ_e) was also obtained from the intercept of the linearized data in the later stage (Fig. 7). Based on the calculations using the geometric approach, the values of k_0, t_{ie}, θ_e, k_a and k_d for the native, heat- and acid-activated bentonite are given in Table 5.
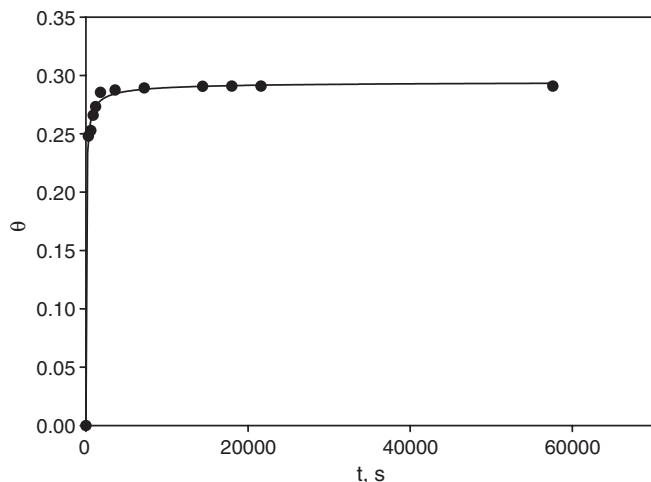
3.7. Calculations of activation energy for adsorption and desorption

Since the k_a and k_d were separately determined, the activation energy of adsorption and desorption can be calculated according to the linear forms of Arrhenius Eqs. (6) and (7). The activation energies were calculated from the slopes of linear regression lines, and the typical
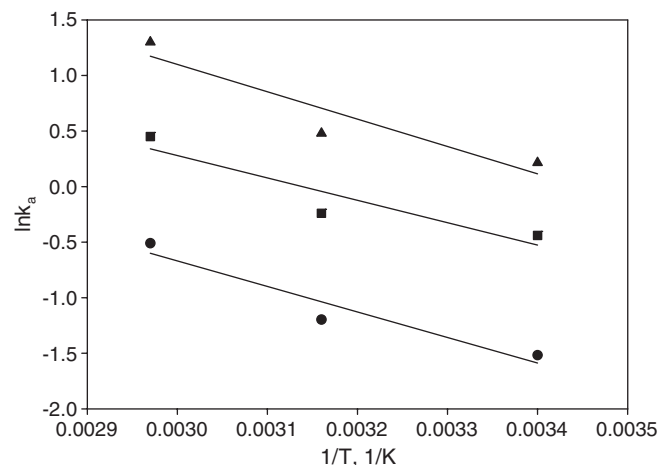

Fig. 7. The typical example of geometric approach of the kinetic data to obtain k_0, t_{ie} and θ_e (8×10^{-3} kg acid-activated bentonite/dm^3 apple juice at 316 K).

Fig. 8. The Arrhenius plot of $\ln k_a$ vs $1/T$ for 2×10^{-3}, 4×10^{-3} and 8×10^{-3} kg acid-activated bentonite/dm^3 apple juice: $\blacklozenge = 2 \times 10^{-3}$ kg, $\blacksquare = 4 \times 10^{-3}$ kg, $\blacktriangle = 8 \times 10^{-3}$ kg.

Table 5
The kinetic parameters of dark coloured compounds adsorption onto native, heat-activated and acid-activated bentonite as determined by geometric approach

m (kg clay)	T (K)	θ_e	k_0 (s^{-1}) $\times 10^{-3}$	t_{ie} (s)	k_a (s^{-1}) $\times 10^{-3}$	k_d (s^{-1}) $\times 10^{-3}$	r^2
2×10^{-3}	296 (N-B)	0.589	1.217	484.140	3.117	1.700	0.984
	296 (H-B)	0.668	1.517	1443.040	4.133	1.483	0.997
	296 (A-B)	0.646	1.133	570.240	3.650	1.233	0.993
	316 (N-B)	0.605	0.217	290.920	0.567	0.267	0.995
	316 (H-B)	0.679	0.383	1741.020	1.167	0.367	0.987
	316 (A-B)	0.628	1.333	471.240	5.033	1.583	0.987
	336 (N-B)	0.587	0.167	3420.540	0.533	0.250	0.998
	336 (H-B)	0.700	0.267	2560.980	0.950	0.233	0.988
	336 (A-B)	0.616	0.117	5387.760	0.567	0.150	0.989
4×10^{-3}	296 (N-B)	0.536	1.433	372.360	4.800	2.483	0.999
	296 (H-B)	0.582	0.367	1608.060	1.367	0.517	0.992
	296 (A-B)	0.510	2.150	236.760	10.783	4.133	0.985
	316 (N-B)	0.538	0.100	5806.860	0.350	0.150	0.996
	316 (H-B)	0.607	0.183	3310.920	0.900	0.233	0.994
	316 (A-B)	0.475	1.917	249.240	13.150	4.233	0.986
	336 (N-B)	0.503	0.083	5992.860	0.417	0.150	0.997
	336 (H-B)	0.542	0.067	8486.160	0.367	0.100	0.977
	336 (A-B)	0.416	0.067	6760.980	0.650	0.167	0.998
8×10^{-3}	296 (N-B)	0.415	1.183	350.760	6.233	3.333	0.998
	296 (H-B)	0.439	0.200	2126.100	1.433	0.533	0.991
	296 (A-B)	0.344	1.967	175.440	20.667	7.467	0.992
	316 (N-B)	0.392	0.050	7450.620	0.350	0.150	0.997
	316 (H-B)	0.412	0.117	3429.120	1.200	0.350	0.996
	316 (A-B)	0.291	1.750	166.140	26.917	8.533	0.991
	336 (N-B)	0.331	0.050	7178.400	0.433	0.183	0.995
	336 (H-B)	0.355	0.017	14477.400	0.317	0.083	0.959
	336 (A-B)	0.236	0.033	6372.480	0.933	0.233	0.998
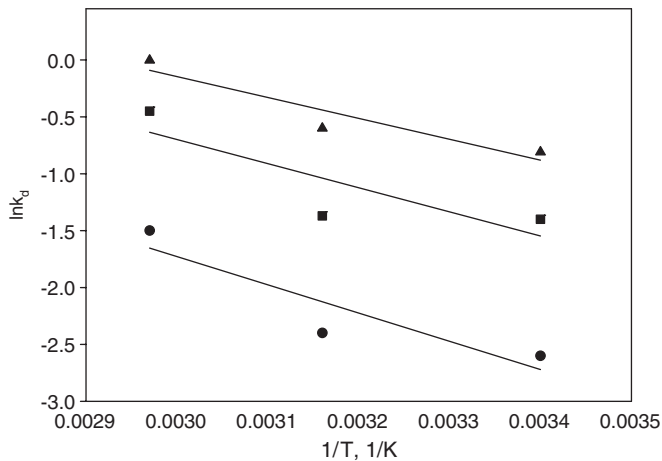
Fig. 9. The Arrhenius plot of $\ln k_d$ vs $1/T$ for 2×10^{-3}, 4×10^{-3} and 8×10^{-3} kg acid-activated bentonite/dm^3 apple juice: $\blacklozenge = 2 \times 10^{-3}$ kg, $\blacksquare = 4 \times 10^{-3}$ kg, $\blacktriangle = 8 \times 10^{-3}$ kg.

Table 6
The activation energies and frequency factors of adsorption and desorption for native, heat-activated and acid-activated bentonite

Bentonite	m (kg clay)	E_a (kJ mol^{-1})	A_a	E_d (kJ mol^{-1})	A_d
Native	2×10^{-3}	35.899	1015.259	37.452	798.312
	4×10^{-3}	33.900	327.766	35.069	233.972
	8×10^{-3}	37.601	1265.978	38.350	882.183
Heat-activated	2×10^{-3}	27.640	63.918	30.199	49.984
	4×10^{-3}	25.858	14.905	29.353	17.542
	8×10^{-3}	28.995	53.543	33.993	108.234
Acid-activated	2×10^{-3}	19.108	8.436	20.650	5.102
	4×10^{-3}	16.765	7.518	17.621	4.786
	8×10^{-3}	20.469	80.761	15.263	3.550

example for acid-activated bentonite is shown in Figs. 8 and 9. It can be said that the activation energy for adsorption and desorption are temperature-sensitive in all the assays (Levenspiel, 1962). The adsorption and desorption rate constants depend both on temperature and clay concentrations. However, the activation energies of adsorption and desorption should be the same for each concentration of bentonite samples. The activation energies of adsorption (E_a) and desorption (E_d) and frequency factors ($A_{a,d}$) for native, heat- and acid-activated bentonite are shown in Table 6.

4. Conclusions

The adsorption of dark-coloured compounds on native, heat- and acid-activated bentonite was an endothermic process, controlled by physical mechanisms, enthalpic-governed and spontaneous. The adsorption efficiency with acid-activated bentonite was greater than that of heat-activated and native bentonite. Increasing the clay

concentrations from 2×10^{-3} to 8×10^{-3} kg clay/dm^3 apple juice also increased the efficiency of adsorption. It is clearly showed that acid-activated bentonite is more suitable for the adsorption of dark-coloured compounds from apple juice. The acid-activated bentonite concentration of 4×10^{-3}–8×10^{-3} kg/dm^3 apple juice, contact time of 300–3×10^3 s with a temperature from 316 to 336 K is enough to clarify the colour of apple juice up to 70–90% for a practical application.

References

Ajmal, M., Rao, R. A. K., Ahmad, R., & Ahmad, J. (2000). Adsorption studies on citrus reticula fruit peel of orange: Removal and recovery of Ni(II) from electroplating wastewater. *Journal of Hazardous Materials*, B79, 117–131.

Artık, N., Cemeroğlu, B., & Aydar, G. (1994). Use of activated carbon for color control in the apple juice concentrate (AJC) production. *Fruit Processing*, 2, 34–39.

Babsky, N. E., Toribio, J. L., & Lozano, J. E. (1986). Influence of storage on the composition of clarified apple juice concentrate. *Journal of Food Science*, 51(3), 564–567.

Barrett, E. P., Joyner, L. G., & Halenda, P. H. (1951). The determination of pore volume and area distributions in porous substance. I. Computations from nitrogen isotherms. *Journal of the American Chemical Society*, 73, 373–380.

Beveridge, T., Franz, K., & Harrison, J. E. (1986). Clarified natural apple juice: Production and storage stability of juice and concentrate. *Journal of Food Science*, 51, 411–414.

Blade, W. H., & Boulton, R. (1988). Adsorption of protein by bentonite in a model wine solution. *American Journal of Enology and Viticulture*, 39, 193–199.

Carabasa, M., Ibarz, A., Garza, S., & Barbosa-Cánovas, G. V. (1998). Removal of dark compounds from clarified fruit juices by adsorption processes. *Journal of Food Engineering*, 37, 25–41.

Constenla, D. T., & Lozano, J. E. (1995). Effect of ultrafiltration on concentrated apple juice colour and turbidity. *International Journal of Food Science and Technology*, 30, 23–30.

Dik, T., Katnaş, S., & Özilgen, M. (1996). Effect of bentonite combinations and gelatin on the rheological behaviour of bentonite–apple juice dispersions. *Lebensmittel-Wissenschaft und-Technologie*, 29, 673–676.

Dik, T., & Özilgen, M. (1994). Rheological behaviour of bentonite–apple juice dispersions. *Lebensmittel-Wissenschaft und-Technologie*, 27, 55–58.

Ekşi, A. (1988). *Fruit juice clarification techniques* (pp. 56–60). Ankara: Gıda Teknolojisi Derneği.

Giovanelli, G., & Ravasini, G. (1993). Apple juice stabilization by combined enzyme-membrane filtration process. *Lebensmittel-Wissenschaft und-Technologie*, 26, 1–7.

Gökmen, V., & Serpen, A. (2002). Equilibrium and kinetic studies on the adsorption of dark colored compounds from apple juice using adsorbent resin. *Journal of Food Engineering*, 53, 221–227.

González, C., Ibarz, A., Esplugas, S., & Vincente, M. (1998). Cinética del pardeamiento no enzimático de zumos de frutas. *Alimentaria*, 198, 53–60.

Günter, S., & Stocké, R. (1995). Schönen von Fruchtsäften (6): Aktivkohle und PVPP. *Flüssiges Obst*, 62, 254–257.

Hums, N., Krug, K., Heess, E., & Storz, H. (1980). Die stabilizierung von apfelsaft mit polyvinylpolypyrrolidone (PVPP) im recycling. *Flüssiges Obst*, 47, 283–287.

Ibarz, A., Casero, T., Miguelsanz, R., & Pagán, J. (1989). Cinética de pardeamiento no enzimático de concentrado de zumo de pera almacenado a distintas temperaturas. *Revista de Agroquimica Tecnologia de Alimentos*, 29(3), 407–414.

Jovanovic, N., & Janackovie, J. (1991). Pore structure and adsorption properties of an acid-activated bentonite. *Applied Clay Science, 6*, 59–67.

Kara, M., Yuzer, H., Sabah, E., & Celik, M. S. (2003). Adsorption of cobalt from aqueous solutions onto sepiolite. *Water Research, 37*, 224–232.

Kuan, W.-H., Lo, S.-L., Chang, C. M., & Wang, M. K. (2000). A geometric approach to determine adsorption and desorption kinetic constants. *Chemosphere, 41*, 1741–1747.

Langmuir, I. (1918). The adsorption of gases on plane surfaces of glass, mica and platinum. *Journal of the American Chemical Society, 40*, 1361–1403.

Lea, A. G. H. (1990). Apple juice. In D. Hicks (Ed.), *Production and packaging of noncarbonated fruit juices and fruit beverages* (pp. 182–225). New York: Blackie and Son.

Levenspiel, O. (1962). *Chemical reaction engineering* (pp. 22–30). USA: Wiley.

McCabe, W. L., Smith, J. C., & Harriott, P. (1993). *Unit operations of chemical engineering* (pp. 810–837) (5th ed.). Singapore: McGraw-Hill.

Özcan, A. S., Erdem, B., & Özcan, A. (2004). Adsorption of acid blue 193 from aqueous solutions onto Na-bentonite and DTMA-bentonite. *Journal of Colloid and Interface Science, 280*, 44–54.

Root, W. H. (1996). Apples and apple processing. In L. P. Somogyi, D. M. Barret, & Y. H. Hui (Eds.), *Processing fruits (vol. 2): Science and technology* (pp. 1–35). Lancaster: Technomic.

Schobinger, U., Barbic, I., Dürr, P., & Waldvogel, R. (1995). Phenolic compounds in apple juice-positive and negative effects. *Fruit Processing, 6*(95), 171–178.

Tahir, S. S., & Rauf, N. (2003). Thermodynamic studies of Ni(II) adsorption onto bentonite from aqueous solution. *Journal of Chemical Thermodynamics, 35*, 2003–2009.

Toribio, J. F., & Lozano, J. E. (1984). Nonenzymatic browning in apple juice concentrate during storage. *Journal of Food Science, 49*, 889–892.

Venaruzzo, J. L., Volzone, C., Rueda, M. L., & Ortiga, J. (2002). Modified bentonitic clay minerals as adsorbent of CO, CO_2 and SO_2 gases. *Microporous and Mesoporous Materials, 56*, 73–80.

Vogt, K. (1987). Neue möglichkeiten in der aufarbeitung von trüben apfelsaftkonzentraten-ultrafiltration und PVPP-stabilisierung-entfärärbung. *Flüssiges Obst, 54*, 425–429.

Weinand, R. (1995). Adsorbent resins in the beverage industry. *Fruit Processing, 6*, 166–170.

Yıldız, N., Aktaş, Z., & Çalımlı, A. (2004). Sulphuric acid activation of a calcium bentonite. *Particulate Science and Technology, 22*(1), 21–23.

Yıldız, N., Gönülşen, R., Koyuncu, H., & Çalımlı, A. (2005). Adsorption of benzoic acid and hydroquinone by organically modified bentonites. *Colloids and Surfaces A: Physicochemical and Engineering Aspects, 260*, 87–94.